Side-Chain Conformation of the M2 Transmembrane Peptide Proton Channel of Influenza A Virus from ^{19}F Solid-State NMR

Wenbin Luo, Rajeswari Mani, and Mei Hong*

Department of Chemistry, Iowa State University, Ames, Iowa 50011

Received: May 17, 2007; In Final Form: July 3, 2007

The M2 transmembrane peptide (M2TMP) of the influenza A virus forms a tetrameric helical bundle that acts as a proton-selective channel important in the viral life cycle. The side-chain conformation of the peptide is largely unknown and is important for elucidating the proton-conducting mechanism and the channel stability. Using a ^{19}F spin diffusion NMR technique called CODEX, we have measured the oligomeric states and interhelical side chain−side chain $^{19}F-^{19}F$ distances at several residues using singly fluorinated M2TMP bound to DMPC bilayers. ^{19}F CODEX data at a key residue of the proton channel, Trp_{41}, confirm the tetrameric state of the peptide and yield a nearest-neighbor interhelical distance of ∼11 Å under both neutral and acidic pH. Since the helix orientation is precisely known from previous ^{15}N NMR experiments and the backbone channel diameter has a narrow allowed range, this ^{19}F distance constrains the Trp_{41} side-chain conformation to *t*90 ($\chi_1 \approx 180°$, $\chi_2 \approx 90°$). This Trp_{41} rotamer, combined with a previously measured $^{15}N-^{13}C$ distance between His_{37} and Trp_{41}[1], suggests that the His_{37} rotamer is *t*−160. The implication of the proposed (His_{37}, Trp_{41}) rotamers to the gating mechanism of the M2 proton channel is discussed. Binding of the antiviral drug amantadine to the peptide does not affect the F−F distance at Trp_{41}. Interhelical $^{19}F-^{19}F$ distances are also measured at residues 27 and 38, each mutated to 4-^{19}F-Phe. For V27F-M2TMP, the $^{19}F-^{19}F$ distances suggest a mixture of dimers and tetramers, whereas the L38F-M2TMP data indicate two tetramers of different sizes, suggesting side chain conformational heterogeneity at this lipid-facing residue. This work shows that ^{19}F spin diffusion NMR is a valuable tool for determining long-range intermolecular distances that shed light on the mechanism of action and conformational heterogeneity of membrane protein oligomers.

Introduction

The determination of the three-dimensional structure of membrane proteins and their assemblies requires long-range intermolecular distances >10 Å. While NMR spectroscopy can readily measure short distances of ∼5 Å accurately, long-range distance measurement remains a challenge.[2] Recently, we have shown ^{19}F spin diffusion to be a robust strategy for obtaining site-specific long-range distances. This approach, termed CODEX, involves measuring dipolar exchange between chemically identical but orientationally different ^{19}F spins on different molecules through a chemical-shift-anisotropy-based stimulated echo.[3−5] Intermolecular $^{19}F-^{19}F$ dipolar couplings in membrane peptide assemblies manifest as a decrease in the stimulated-echo intensity as a function of the exchange mixing time. The intensity decay is then fit to yield distances up to 15 Å with an uncertainty of 0.5−1.0 Å.[6,7] Both the number of spins in the cluster and internuclear distances can be obtained from the time-dependent echo decay curve.

The M2 protein of influenza A virus is a tetrameric proton channel essential in the life cycle of the virus. The channel is closed at neutral pH but opens in the acidic environment (low pH_{out}) of the endosome after viral entry into the host cell.[8,9] The acidification of the viral interior initiates the release of the viral RNA into the host cell, causing infection. Binding of amantadine blocks the proton channel and prevents infection. Elucidating the structure of the M2 proton channel in the closed and open states is thus important for understanding the mechanism of proton transfer and for designing antiviral drugs. Electrophysiological measurements on the M2 protein and analytical ultracentrifugation (AUC) experiments on the transmembrane domain of the M2 protein, M2TMP, have unambiguously established that His_{37} is the key residue for proton conductance.[10−12]

In addition to His_{37}, Trp_{41} is another residue known to be important for the proton channel function.[9,13] However, there are two different models about its specific role in M2 proton conductance. The first model was derived from electrophysiological measurements showing that the replacement of Trp_{41} by Phe causes an outward proton current when pH_{out} is high and pH_{in} is low, a condition under which the wild-type channel shows no outward proton flow.[13] This observation led to the conclusion that Trp_{41} is the gate of the channel, such that replacement by amino acids with smaller side chains causes channel leakage. The proposed mechanism for channel gating by Trp_{41} involves conformational changes of the indole ring between the closed and open states: in the closed state it may obstruct the pore while in the open state it may become parallel to the pore axis, allowing the protons to flow inward.

The second model for the role of Trp_{41} in M2TMP resulted from pH-dependent UV resonance Raman spectra:[14] analysis of the wavenumbers and relative peak intensities indicated that there is no change in hydrogen bonding, environmental hydrophobicity, and side-chain torsion angles of the indole ring between the closed and open states.[14] Instead, based on spectral intensity changes, it was suggested that the only change is the

* Address correspondence to this author. Phone: 515-294-3521. Fax: 515-294-0105. E-mail: mhong@iastate.edu.

10.1021/jp073823k CCC: $37.00
Published on Web 08/17/2007

addition of weak cation−π interactions between protonated His_{37} imidazole rings and Trp_{41} in the open state.

Because of the importance of His_{37} and Trp_{41} for proton conductance of the M2TMP channel, distance experiments and molecular dynamics (MD) simulations have been carried out to probe the side-chain conformation of these two residues. Solid-state NMR measurements of the His_{37} Nδ−Trp_{41} Cγ distance suggested (t−160, t−105) rotamers for the (χ_1, χ_2) angles of (His_{37}, Trp_{41}) adduct[1] (PDB: 1NYJ). The *t*−105 rotamer of Trp_{41} points the indole rings toward the pore lumen, which was interpreted as supporting the first, Trp gating, model. However, MD simulations scanning the full conformational space of the two residues subject to this distance restraint proposed an alternative possibility, (t60, t90), that is energetically more stable than the (t−160, t−105) rotamers.[15]

In this work, we probe the side-chain conformation of Trp_{41} in the closed and open states by measuring the interhelical side chain−side chain distances between 5-^{19}F-Trp_{41} using ^{19}F spin diffusion NMR. We find that Trp_{41} has an interhelical nearest-neighbor F−F distance of 11 ± 1 Å at both neutral (closed) and low (open) pH, which constrains the Trp rotamer unambiguously to *t*90. Amantadine binding does not change the interhelical distance at this site. This Trp conformation implies that the His_{37} rotamer is *t*−160 when the previously measured His-Trp distance[1] is considered. We also measured the F−F distances at residues 27 and 38, which are mutated to 4-^{19}F-Phe. We find that both sites show distance heterogeneity, which we attribute to oligomeric mixtures in one case and side-chain conformational distribution in the other. The ^{19}F spin diffusion NMR method is thus sensitive to the conformational heterogeneity of this transmembrane proton channel.

Experimental Methods

NMR Samples. 5-^{19}F-Trp was purchased from BioCatalysts (Pasadena, CA), Fmoc-protected by SynPep Corp. (Dublin, CA), and purified with silica gel column chromatography. 1,2-Dimyristoyl-*sn*-glycero-3-phosphocholine (DMPC) was obtained from Avanti Polar Lipids (Alabaster, AL). The ^{19}F-labeled wild-type and mutant M2TMP samples were custom-synthesized by PrimmBiotech (Cambridge, MA) using standard Fmoc chemistry. The amino acid sequence of the Udorn strain of the influenza A virus is used in most experiments: NH_2-Ser_{22}-Ser_{23}-Asp_{24}-Pro_{25}-Leu_{26}-Val_{27}-Val_{28}-Ala_{29}-Ala_{30}-Ser_{31}-Ile_{32}-Ile_{33}-Gly_{34}-Ile_{35}-Leu_{36}-His_{37}-Leu_{38}-Ile_{39}-Leu_{40}-Trp_{41}-Ile_{42}-Leu_{43}-Asp_{44}-Arg_{45}-Leu_{46}-COOH. The purity of all peptides was checked by HPLC and mass spectrometry to be greater than 95%. The purified peptide was washed in 5 mM HCl solution to remove residual trifluoroacetate (TFA) ions from the synthesis, and checked by solution ^{19}F NMR. The ^{19}F spectra of the membrane-bound peptides contain no detectable TFA signal, indicating complete removal of TFA.

Large unilamellar DMPC vesicles were prepared by dissolving DMPC lipids either in a phosphate buffer (10 mM Na_2HPO_4/NaH_2PO_4, pH 7.5, 30 °C) or in a 10 mM citrate buffer (pH 4.5, 30 °C). The DMPC solution was freeze−thawed 8 times. Purified wild-type and mutant M2TMP peptides were dissolved in the DMPC solution at a peptide−lipid molar ratio (P/L) of 1:15. This P/L value is sufficiently high to promote complete tetramerization of the M2TMP, as shown by analytical ultracentrifugation data.[16] The peptide−lipid mixture was vortexed for 30 min and incubated at 30 °C for 2 days. The solution was ultracentrifuged at 150 000 g for 3 h at 28 °C. This yielded 90% reconstitution of the peptide, as measured by the BCA assay.[17] The pH of the membrane samples was measured through the supernatant to be 7.5 and 4.5 for the phosphate buffer samples and the citrate buffer samples, respectively. The wet membrane pellet was transferred to a 4 mm rotor with borosilicate glass spacers and incubated at 30 °C for 2 days before the NMR experiments. To calculate the peptide molar concentrations of the NMR samples for comparison with the AUC data acquired on DPC micelles, the incubation and ultracentrifugation solution volume of 4 mL was used, giving a M2TMP concentration of ∼0.6 mM.

To assess whether the oligomeric structure and side chain conformation of the peptide are affected by the membrane reconstitution protocol, we also used two other methods to mix the peptide with the lipids and measured the ^{19}F CODEX spectra of the corresponding samples to compare with the aqueous-mixed samples. One method involved cosolubilizing M2TMP with DMPC lipids in chloroform to obtain a well-mixed clear solution. The mixture was dried under a stream of N_2 gas, lyophilized, then rehydrated to 35% water. A Trp_{41}-M2TMP sample was prepared in this way. The third method codissolves M2TMP in the detergent octyl-β-glucoside (OG) in aqueous buffer (10 mM Na_2HPO_4/NaH_2PO_4, 1 mM EDTA) with the desired pH.[18,19] The clear solution was then mixed with a DMPC vesicle solution to reach an OG concentration of 10% and a P/L of 1:15. The detergent was then removed by dialysis against the 10 mM Na_2HPO_4/NaH_2PO_4 buffer at 4 °C for 3 days. The dialyzed peptide−lipid solution was centrifuged to give the pellet for solid-state NMR experiments. The absence of detergent in the peptide−lipid mixture was confirmed by ^{1}H solution NMR on the supernatant from ultracentrifugation. A V27F-M2TMP sample was prepared in this way to compare with the aqueous mixed sample. The amantadine-bound Trp_{41}-M2TMP sample was also prepared by the detergent dialysis method, where 10 mM amantadine was added to the DMPC vesicle solution and the dialysis buffer solution.

Solid-State NMR Experiments. The ^{19}F CODEX experiments were carried out on a Bruker DSX-400 spectrometer (Karlsruhe, Germany) operating at a resonance frequency of 400.49 MHz for ^{1}H and 376.8 MHz for ^{19}F, using an H/F/X probe equipped with a 4 mm MAS spinner module. The probe tunes ^{1}H and ^{19}F frequencies on a single channel. Experiments on M2TMP were conducted at 8 kHz MAS and 233 K, using air cooled by a Kinetics Thermal Systems XR Air-Jet cooler (Stone Ridge, NY). Typical radio frequency (rf) field strengths were 50 kHz for ^{19}F and ^{1}H. Recycle delay was 1.5 s. ^{1}H−^{19}F cross-polarization (CP) contact times were 200 μs. ^{19}F chemical shifts were externally referenced to the Teflon ^{19}F signal at −122 ppm.

The ^{19}F CODEX experiment uses two rotor-synchronized π-pulse trains to recouple the chemical shift anisotropy (CSA).[4] The mixing time (τ_m) between the two trains allows spin diffusion to occur, which changes the CSA frequency and prevents complete refocusing of the stimulated echo. To correct for ^{19}F spin−lattice relaxation (T_1) effects during the mixing time τ_m, a *z*-filter (τ_z) is added at the end of the second π-pulse train. Two experiments were conducted: a dephasing experiment (S) with the desired τ_m and a short τ_z of 10 μs, and a reference experiment (S_0) with interchanged τ_m and τ_z values. The normalized echo intensity, S/S_0, decays to $1/n$ at long mixing times for an *n*-spin cluster. All CODEX experiments were conducted with two rotor periods (τ_r) of CSA recoupling. This resulted in $2\pi\delta N\tau_r$ values from 9π to 12π, where δ is the chemical shift anisotropy of the ^{19}F label. These values were sufficiently large to detect small orientational differences between different helices in the tetramer.[5]

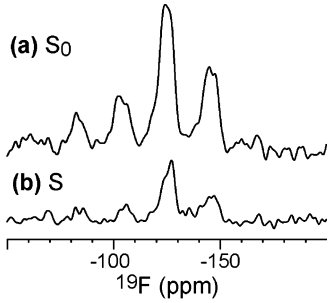

Figure 1. ^{19}F CODEX spectra of [5-^{19}F-Trp$_{41}$] M2TMP in DMPC bilayers at pH 7.5. The mixing time is 3.0 s. Data were collected at 233 K under 8 kHz MAS. (a) Reference spectrum S_0 to correct for T_1 relaxation effects. (b) Dephasing spectrum S. The normalized intensity S/S_0 is 0.36 ± 0.04.

CODEX Data Analysis. The CODEX magnetization exchange curves were calculated in MATLAB with use of an exchange-matrix formalism.[6] Four-dimensional exchange rate matrices were constructed for the tetrameric bundle, where the rate constants are proportional to an overlap integral, $F(0)$, and to the square of the dipolar couplings, ω_{FF}, which depend on the F−F distances. Thus all distance contacts in the four-spin cluster, including the nearest-neighbor distances and the diagonal distance, are included in the matrix. Our recent model compound studies yielded an $F(0)$ of 37 μs for aromatic ^{19}F sites under identical MAS conditions as used here.[6] Thus, we fix this value and vary ω_{FF} to find the best-fit spin diffusion curve. The best-fit curve is evaluated by minimizing the root-mean-square derivation (rmsd) between the calculated intensity I_{sim} and the experimental intensity I_{exp}. The interhelical nearest-neighbor F−F distances determining the coupling strengths were incremented at 0.1 Å steps.

Structure Modeling. M2TMP structure was modeled in Insight II (Accelrys, San Diego). The structural model 1NYJ[1] of Cross and co-workers was used as the starting point and was modified to satisfy the ^{19}F CODEX data. We specify the side chain conformations of His$_{37}$ and Trp$_{41}$ using the notation of the penultimate rotamer library.[20] The χ_1 angle is specified as t, p, or m, corresponding to 180°, +60°, and −60°, respectively. These letters are followed by the approximate numerical value of the χ_2 angle. Thus, for example, the His$_{37}$ and Trp$_{41}$ conformations in the 1NYJ model are (t−160, t−105).[1,15]

Results

Interhelical F−F Distance at Trp$_{41}$ at Neutral and Acidic pH. Trp$_{41}$ is recognized to be an important residue in M2TMP function, and has been proposed to act as the gate of the channel.[9,13] Thus, we used 5-^{19}F-Trp$_{41}$ to measure the interhelical side chain−side chain F−F distances in this part of the peptide assembly. Figure 1 shows a representative pair of CODEX spectra of 5-^{19}F-Trp$_{41}$ M2TMP in DMPC bilayers at pH 7.5, acquired with a mixing time of 3.0 s under 8 kHz MAS and at 233 K. Significant dephasing, with $S/S_0 = 0.36$, of the S spectrum is observed compared to the reference spectrum S_0, indicating the presence of multiple peptides with orientationally different ^{19}F chemical shift tensors in close proximity. The M2TMP helical bundle is known to be pseudosymmetric,[21] but the symmetry is rotational rather than translational, thus the ^{19}F chemical shift tensor orientations differ significantly between the helices in the assembly, allowing the detection of this CODEX effect.

The complete mixing-time dependent CODEX curve of 5-^{19}F-Trp$_{41}$ is shown in Figure 2. The final normalized intensity is

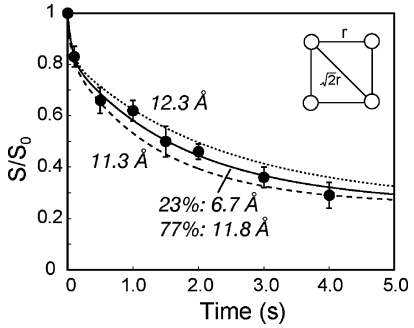

Figure 2. Normalized ^{19}F CODEX intensity of 5-^{19}F-Trp$_{41}$ M2TMP in DMPC bilayers at pH 7.5. Error bars were propagated from the spectral sensitivity. In the CODEX simulation, an overlap integral $F(0)$ of 37 μs was used. Bimodal fitting using a 23% component of a 6.7 Å distance and 77% of an 11.8 Å distance best fits the double exponential decay of the experimental intensities.

0.29 ± 0.05, observed at a mixing time of 4.0 s, confirming the tetrameric state of the peptide in DMPC bilayers. Longer mixing times were not measured because spectral intensities become prohibitively low due to ^{19}F spin−lattice relaxation (T_1 = 3.2 s). A separate sample prepared by using organic-phase mixing of the lipid and peptide gave the same CODEX decay curve as the aqueous-mixed sample (Supporting Information Figure S1), indicating that the aqueous-mixed sample gives structurally identical tetramers as the organic samples. The only difference is that aqueous mixing produces more immobilized peptides than organic mixing,[22] thus facilitating the CODEX experiment, which requires that reorientation motion be frozen during the mixing time.

The equilibrium value of 0.29 for Trp$_{41}$ gives an upper bound to the fraction of possible monomer in the sample: 10% monomer would give an equilibrium value of 0.33 (=10% × 1 + 90% × 0.25), which is distinguishable from the experimental data. Thus any monomer component, if present, is no more than 10%, and the Trp$_{41}$-M2TMP sample is predominantly tetrameric in DMPC bilayers.

To fit the Trp$_{41}$ CODEX data, we use an exchange-matrix formalism, where the magnetization decay with time is dictated by an exponential rate matrix in which the rate constants depend on the distance-dependent dipolar couplings and a spectral overlap integral $F(0)$. Using an overlap integral value of 37 μs,[6] which was calibrated by experiments on model compounds under the same MAS conditions, we find a nearest-neighbor distance of 11.2 ± 0.5 Å using a single symmetric 4-spin model (Supporting Information Figure S2a). The presence of the diagonal distance between nonadjacent helices is automatically taken into account in the 4 × 4 exchange matrix. However, the single-tetramer fit does not capture well a minor component of fast initial decay in the experimental data. Thus we simulated the data with a double-tetramer model where the two tetramers have different side lengths. The fraction of each tetramer was obtained from the height of the turning point between the fast and slow decays. Figure 2 shows that a 23% component with a short nearest-neighbor F−F distance of 6.7 Å and a 77% component with a longer distance of 11.8 ± 0.5 Å best-fit the experimental data. The rmsd analysis is shown in Supporting Information Figure S2b. Since the fraction of the short-distance component is low, below we analyze only the major conformer.

The intermolecular side chain−side chain ^{19}F−^{19}F distances between 5-^{19}F-Trp$_{41}$ residues depend on the orientation of the helices, the pore diameter, and the side chain conformation of Trp$_{41}$. The tilt angle of M2TMP in DMPC bilayers has been determined to be 35 ± 3° by ^{15}N NMR.[21] The rotation angle is

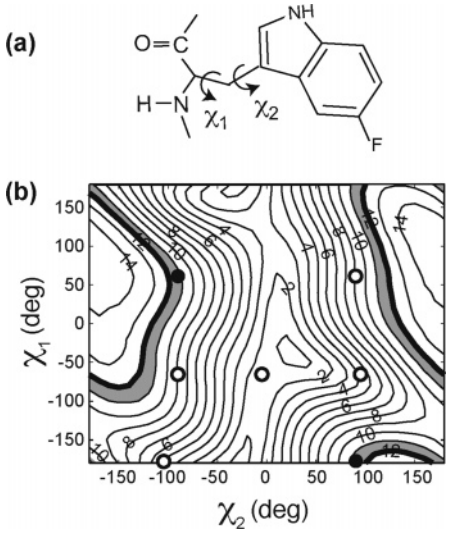

Figure 3. Nearest-neighbor intermolecular $^{19}F-^{19}F$ distance between 5-^{19}F-Trp$_{41}$ as a function of torsion angles χ_1 and χ_2. (a) Definition of the χ_1 and χ_2 torsion angles. (b) Contour plot of the nearest-neighbor F−F distance as a function of (χ_1, χ_2). Circles: Rotameric states of Trp residue in α-helical proteins.[20] Open circles: Rotamers that are ruled out based on the measured F−F distance. Filled circles: Rotameric states allowed by the measured F−F distance. Shaded region: The experimentally measured F−F distance including experimental uncertainty.

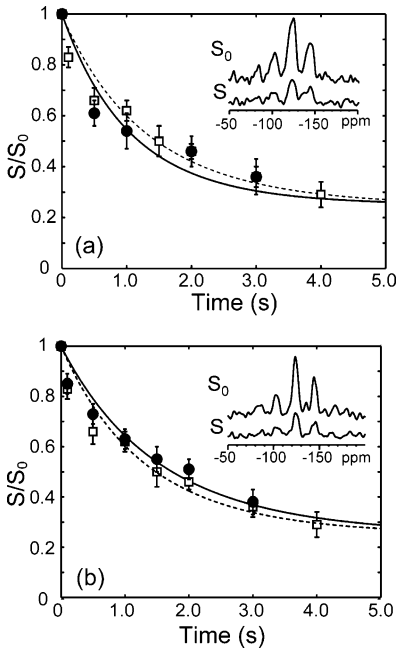

Figure 4. ^{19}F CODEX data of 5-^{19}F-Trp$_{41}$ M2TMP in DMPC bilayers (a) at pH 4.5 (solid circles) and (b) with amantadine bound (solid circles). In both plots the data of the amantadine-free sample at pH 7.5 are shown as open squares for comparison. The S_0 and S spectra at a mixing time of 3.0 s are shown in the insets. (a) The best fit of the pH 4.5 data using a single tetramer model gives a nearest-neighbor F−F distance of 10.8 Å (solid line). This is the same as the pH 7.5 result (dashed line) within experimental uncertainty. (b) The best fit of the amantadine-bound data using a single tetramer model gives a nearest-neighbor F−F distance of 11.5 Å (solid line). This is the same as the amantadine-free data (dashed line) within experimental uncertainty.

also known with high precision. Thus, the peptide orientation is fixed. The pore diameter, indicated by the diagonal Cα−Cα backbone−backbone distance at the central residue Gly$_{34}$, has not been experimentally determined. However, statistical analysis of four-helix-bundle proteins indicates that tetrameric pores have remarkably consistent diameters of 10.0−10.5 Å.[23] For M2TMP, various models derived from experimental data[12] and converged MD simulations[24,25] also put the pore diameter at 10.0−10.5 Å. This small variability likely reflects the requirement of tetramer stability. With this consideration, we used the NMR-derived 1NYJ structure as the starting point of our modeling since it has both the correct orientation and a suitable pore diameter of 10.2 Å for the Gly$_{34}$ Cα−Cα diagonal distance.

These considerations leave the Trp$_{41}$ side-chain conformation as the main parameter influencing the inter-helical side chain−side chain $^{19}F-^{19}F$ distance. Indeed, the χ_1 and χ_2 angles, defined in Figure 3a, change the F−F distance dramatically from 2 Å to 14 Å (Figure 3b). The (χ_1, χ_2) combinations that give a nearest-neighbor F−F distance of 11−12 Å are highlighted as gray areas in Figure 3b. The seven rotamers of Trp populated in α-helical proteins are superimposed as circles in this distance plot.[20,26] As can be seen, only two out of seven rotamers, t90 and p−90, agree with the experimental data (solid circles), thus constraining the conformation of Trp$_{41}$ in the closed state to one of these two possibilities. Even when the variability of pore diameter is taken into account, the F−F distance cannot change by more than ±0.5 Å, which is already included in the experimental uncertainty.

To determine whether low pH corresponding to the open state of the channel changes the side-chain conformation of Trp$_{41}$, we measured the ^{19}F CODEX curve of 5-^{19}F-Trp$_{41}$ labeled M2TMP in DMPC bilayers at pH 4.5. Figure 4a shows that the low pH data (solid circles) overlap with the pH 7.5 data (open squares) within experimental uncertainty. The best-fit distance with a single tetramer model is 10.8 ± 1.0 Å (solid line) based on rmsd analysis (Supporting Information Figure S3). Although the best-fit distance is 0.4 Å shorter than the single-tetramer fit for the neutral pH data, the distance error bar and the CODEX intensity error bars both overlap with those of the pH 7.5 data, therefore within experimental uncertainty there is no detectable difference in the Trp$_{41}$ F−F distances between the neutral and low pH states.

To assess the effect of the antiviral drug amantadine on the Trp$_{41}$ side-chain conformation, we also measured the ^{19}F CODEX intensities of amantadine-bound M2TMP in DMPC bilayers at pH 7.5. Amantadine binding at neutral pH is known to prevent proton conductance and channel opening.[9,27] The CODEX curve of the amantadine-bound Trp$_{41}$ sample is shown in Figure 4b. The data are best-fit with a distance of 11.5 Å by using a single-tetramer model. This is again similar to the 11.2 Å distance of the amantadine-free peptide within experimental uncertainty. The lack of distance change is consistent with the fact that the amantadine binding site is known to be at the N-terminus of the channel,[28] whereas Trp$_{41}$ lies at the C-terminus, on the opposite side of Gly$_{34}$, which is the narrowest point of the tetramer. Thus amantadine binding is not expected to affect the local side-chain conformation of Trp$_{41}$ but at most only indirectly affects the interhelical distances through small changes in the helix tilt angle. Moreover, since the amantadine-bound membrane sample is prepared with the detergent dialysis method, the similar distance with the aqueous-mixed samples further indicates the independence of the tetramer structure on the sample preparation protocol.

Interhelical F−F Distances at V27F and L38F at Neutral pH. To investigate the intermolecular packing of the M2TMP helical bundle at other residues, we mutated V27 and L38 to 4-^{19}F-Phe and measured their CODEX curves. These positions were chosen based on previous AUC data showing that the helical bundle stability is not significantly altered by mutation to Phe. V27 is located at the *a* position of the heptad repeat

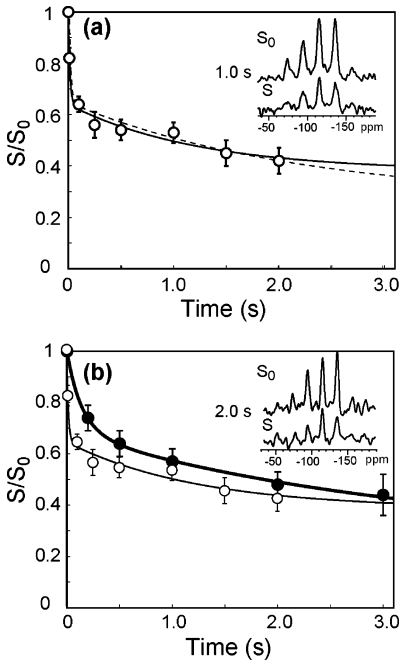

Figure 5. ^{19}F CODEX data of V27F- and L38F-M2TMP in DMPC bilayers at pH 7.5. (a) 4-^{19}F-Phe labeled V27F-M2TMP. The best fit using a dimer−tetramer mixture (solid line) gives a distance of 10.5 and 5.3 Å (nearest-neighbor distance) for the dimer and tetramer at a weight ratio 52:48. Best fit using a tetramer−tetramer mixture (dashed line) gives distances of 12.3 and 5.3 Å at a ratio of 52:48. (b) 4-^{19}F-Phe labeled L38F-M2TMP (filled circles). The best fit gives two tetramers with side lengths of 13.1 and 7.7 Å at a ratio of 58:42. The V27F data are reproduced in part b for comparison. Data were obtained at 233 K under 8 kHz MAS. Representatives of S_0 and S spectra are shown in the insets.

and faces the pore lumen, thus is expected to have a short interhelical distance. In comparison, L38 lies at the *e* position of the heptad repeat and is expected to point to the lipid−peptide interface. The L38F mutant is also found in nature in the Weybridge strain of influenza A virus: this proton channel has amantadine sensitivity[27] similar to the Udorn strain studied in the rest of this paper. Thus, the L38F mutation is expected to be particularly nonperturbing to the tetramer structure.

Figure 5 shows the CODEX data of V27F-M2TMP and L38F-M2TMP in DMPC bilayers at pH 7.5. The V27F curve decays quickly in the first 500 ms, then appears to plateau to ∼0.40 by 2.0 s. The same decay trend is reproduced in a detergent-dialysis sample (Supporting Information Figure S1). In comparison, the L38F intensity decays more slowly and at the longest mixing time used (3.0 s) the intensity continues to decrease. The different decay rates between the initial and final parts of the V27F data suggest a distribution of distances. We first used a model of two tetramers with different distances to fit the V27F data. Figure 5a shows that a mixture of 52% of a tetramer with a side length of 12.3 Å and 48% of a tetramer with a side length of 5.3 Å fits the data well (Figure 5a, dashed line). Since the pore diameter is unlikely to change by more than 1 Å, the very different distances would mean that Phe_{27} adopts different χ_1 angles, with −100° and −160° for the long and short distances, respectively (Supporting Information Figure S6a).

However, the relatively high final value of ∼0.4 and the apparent plateau at long mixing times suggest an alternative interpretation where the V27F mutant forms a mixture of dimers and tetramers in DMPC bilayers. Thus we simulated the CODEX data using varying fractions of dimers and tetramers. A model where 52% of the peptide is in a dimer state with an intermolecular distance of 10.5 Å and 48% of the peptide is in a tetramer state with a nearest-neighbor interhelical distance of 5.3 Å captures the experimental data best (Figure 5a, solid line). The rmsd plot for the simulation is shown in Supporting Information Figure S4a. Increasing the dimer fraction to as much as 70% still gave acceptable fits while using less than 50% dimer fraction disagrees with the data (Supporting Information Figure S5). This suggests that V27F-M2TMP may be at least half populated as dimers while the rest are well-defined tight tetramers. The tetramer distance of 5.3 Å would be satisfied by the t80 conformer, which is the most populated rotamer of Phe in α-helices[20,26] (Supporting Information Figure S6a).

The L38F CODEX curve shows a clearer decay trend through the 3.0 s mixing time, suggesting that the data can be fit straightforwardly with tetramers only. But similar to the V27F sample, a single distance does not fit the data well, but two distances of 13.1 (58%) and 7.7 Å (42%) for the tetramer side lengths give excellent fit to the data (Figure 5b, with the rmsd plot in Supporting Information Figure S4b). Weight fractions differing by more than 15% from the best-fit fractions can be ruled out on physical grounds (Supporting Information Figure S5c). The longer distance of 13.1 Å translates to a Phe_{38} rotamer of t80 (58%),[20,26] whereas the shorter distance indicates a χ_1 angle of about −130° (42%) (Supporting Information Figure S6). The latter rotamer, although noncanonical, is still found in Phe residues in proteins.[26]

Discussion

Trp_{41} Side-Chain Conformation. Interhelical F−F distances between 5-^{19}F-Trp_{41} labeled M2TMP have been measured in three states: the neutral pH, the low pH, and the amantadine-bound neutral pH states. All three samples exhibit nearest-neighbor distances between 10.8 and 11.8 Å, with uncertainties of ±0.5 to ±1.0 Å. We first consider the neutral pH amantadine-free state. The 11.8 ± 1.0 Å distance obtained for the major conformer is a strong constraint of the Trp side-chain conformation. The existing model (1NYJ) put the Trp_{41} rotamer as t−105, based on a measured His_{37} Nδ−Trp_{41} Cγ distance of <3.9 Å.[1] However, this would give rise to a F−F distance of 5.1 Å (Figure 3b and Figure 6b), in clear disagreement with the current ^{19}F data. Instead, the measured F−F distance restrains the Trp_{41} conformation to either t90 ($\chi_1 \approx 180°$, $\chi_2 \approx 90°$) or p−90 ($\chi_1 \approx +60°$, $\chi_2 \approx -90°$) (solid circles in Figure 3b). The $\chi_1 = 60°$ (p) rotamer causes steric conflicts between the indole ring and the Cα of residue Leu_{38} and thus is rarely populated in α-helices (2%).[20,26] In contrast, the t90 rotamer is one of the most populated rotamers of Trp in α-helices.[20,26] Thus, we propose the t90 rotamer for Trp_{41}.

The t90 rotamer of Trp_{41} for both the closed and open states is in excellent agreement with a number of observations from the UV resonance Raman spectra of Takeuchi and co-workers.[14] First, the wavenumber of the W3 peak in the Raman spectra predicted a χ_2 angle of around 100°, in agreement with the current result. Second, the W7 peak intensity, which reflects the environmental hydrophobicity of the indole ring, and the W3 wavenumber, a marker of the absolute value of χ_2, both showed little change between the open and closed states, suggesting that Trp_{41} side chain conformation is similar between the open and closed states. This is consistent with the observed lack of change in the F−F distance between high and low pH (Figure 4). Therefore, even though the importance of Trp_{41} in proton conductance is unambiguous, the detail of Trp's role in gating is more subtle and does not appear to involve the large conformational change hypothesized by Tang et al.[13]

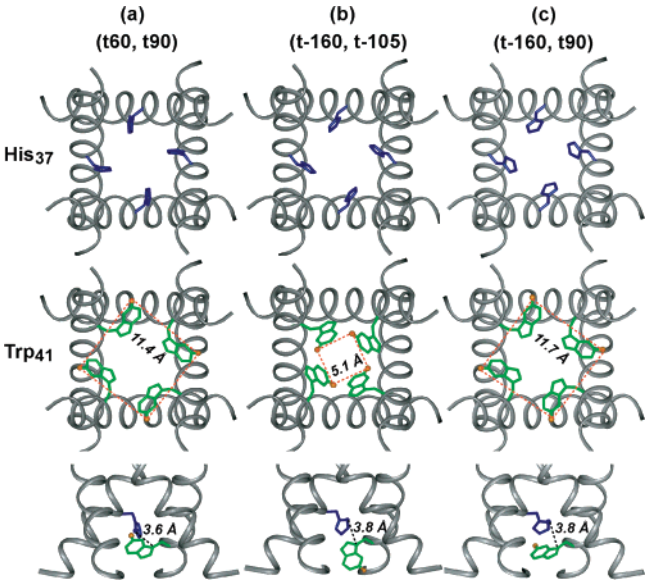

Figure 6. ^{19}F NMR restrained conformation of Trp_{41} and His_{37} in M2TMP in DMPC bilayers. Top row: His_{37} (blue) in the top view of the channel from the C-terminus to the N-terminus. Middle row: Trp_{41} (green) and the F−F distance (orange). Bottom row: side view of the channel showing both Trp_{41} and His_{37} and the Cγ−Nδ distance between them. The (His_{37}, Trp_{41}) side chain conformation is (a) (t60, t90), (b) (t−160, t−105), and (c) (t−160, t90). The structure labeled a disagrees with the C−N distance data[1] due to unfavorable orientation of the C−N vector, whereas the structure labeled b disagrees with the F−F distance data. Only the structure labeled c satisfies both constraints.

Implications of the Trp_{41} Conformation to His_{37} Conformation. Fixing the Trp_{41} conformation to t90 and varying the His_{37} conformation, we find two His_{37} rotamers, t60 and t−160, that give a His_{37} Nδ−Trp_{41} Cγ distance within the experimental range of <3.9 Å measured by Cross and co-workers. However, the t60 rotamer of His_{37} in combination with a Trp_{41} t90 rotamer gives an Nδ−Cγ bond orientation close to the magic angle relative to the helical bundle axis (Figure 6a), thus the fast uniaxial rotation of the tetrameric helical bundle[22] would significantly average the Nδ−Cγ dipolar coupling to much less than the experimental value of 63 ± 12 Hz.[1] In contrast, the t−160 conformation of His_{37} in combination with the Trp_{41} t90 rotamer gives an Nδ−Cγ vector that is roughly parallel to the bundle axis (Figure 6c), thus is consistent with the measured motionally averaged C−N dipolar coupling. Thus, we propose the (t−160, 90) conformation for (His_{37}, Trp_{41}) (Figure 6c).

Wu and Voth carried out a MD simulation that examined the Nδ−Cγ distances in four possible (His_{37}, Trp_{41}) adducts and proposed the (t60, t90) rotamer pair.[15] The t90 rotamer for Trp_{41} agrees with the current ^{19}F distance data; however, the t60 rotamer for His_{37} is suspect. The MD simulations used a helical tilt angle of 30°, which is significantly lower than the experimental value, and the His37 χ_2 angle that reproduced the Nδ−Cγ distance constraint in the simulation is 110°, which is 50° away from the ideal value of 60°. When the ^{15}N NMR extracted tilt angle of 38° is used and the His χ_1 and χ_2 angles are kept within 20° of the ideal values, we find the t60 rotamer of His_{37} to no longer give a suitable Nδ−Cγ dipolar coupling of 63 ± 12 Hz.

The (t−160, t90) rotamer pair we propose was previously overlooked by Cross and co-workers for steric reasons. However, within ±20° of the ideal torsion angle values, the two residues in this rotamer combination maintain a minimum separation of 3.3 Å between the imidazole ring and indole ring

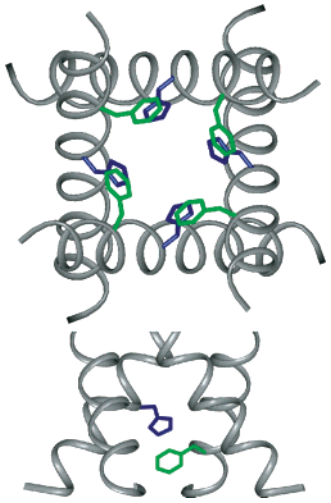

Figure 7. Proposed conformation of W41F mutant of M2TMP and the His_{37} contact with Phe_{41}. Only the neutral pH_{out} state is considered. Top row: Top view of M2TMP from the C-terminus to the N-terminus. Bottom row: Side view. His_{37} is in the *t*−160 state and Phe_{41} is in the most populated *t*80 state. The two rings are further away from each other than in Figure 6c.

while still satisfying the F−F and C−N distance constraints (Figure 6c). Thus, steric conflict is not a problem for this rotamer pair.

To prove beyond doubt the side-chain conformation of His_{37}, rigid-limit dipolar couplings in the absence of complicating motions need to be measured. The previous C−N distance measurement was conducted at 38 °C, well into the liquid-crystalline phase of the DMPC bilayer. At this temperature, the His_{37} Nδ position is influenced by (χ_1, χ_2) torsional motions in addition to the uniaxial whole-body rotation of the helical bundle. These multiple degrees of freedom average the dipolar coupling in a complicated fashion and cannot be adequately taken into account in the distance extraction. The mobility of the peptide in the liquid-crystalline phase does not, however, affect the helix orientation measurement on glass-plate samples, since these samples used backbone ^{15}N-labeled peptides, whose uniaxial rotation around the bilayer normal or the magnetic field is invisible in the spectra.[21]

The Implication of the Trp_{41} Conformation to the Gating Mechanism. How do the Trp_{41} side-chain conformation and the proposed (His_{37}, Trp_{41}) rotamer pair explain the observed proton blockage in the closed state and proton conduction in the open state, given the fact the Trp_{41} 5-^{19}F interhelical distance remains largely unchanged at ~11 Å between neutral and acidic pH? We propose two models. In the first model, the (t−160, t90) rotamer pair places the His_{37} imidazole rings close to the Trp_{41} indole rings (Figure 6c). Thus when pH_{in} is low and pH_{out} is high, the C-terminal indole rings prevent the intracellular protons from protonating His. The His rings occlude the pore, either by formation of imidazole−imidazolium dimers[29] or sterically. When pH_{out} is low and pH_{in} is high, the extracellular protons from the N-terminus are able to protonate all four imidazole rings. This either results in electrostatic repulsion that opens the constriction at His_{37}, or causes the excess proton on the imidazolium ion to be relayed as His returns to its neutral state.[9,29] When Trp_{41} is mutated to Phe, the phenylene ring, in its most populated rotamer of t80, is further away from the imidazoles (Figure 7), thus allowing protons to protonate His_{37} from either direction, causing a leaky channel.[13] Thus, in this model, close proximity and interaction between Trp_{41} and His_{37} combined with the constriction at His_{37} gate the channel.

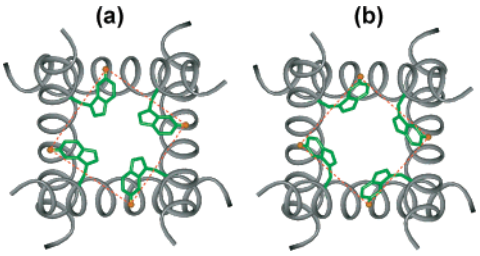

Figure 8. Two Trp_{41} t90 conformations that satisfy the ^{19}F CODEX distance constraint while changing the pore constriction. (a) $\chi_1 = -157°$ and $\chi_2 = 110°$. The pore constriction, indicated by the shortest diagonal proton−proton van der Waals distance, is 2.2 Å, and the F−F nearest-neighbor interhelical distance is 11.4 Å. (b) $\chi_1 = -177°$ and $\chi_2 = 80°$. The pore constriction is 4.8 Å while the F−F nearest-neighbor interhelical distance is 10.7 Å.

Examination of the pore constrictions at Trp_{41} and His_{37} raises a second possibility for channel gating. At the t90 Trp_{41}, the shortest diagonal distance between protons of the indole rings is 2.2−6.5 Å, after taking into account the hydrogen atom van der Waals radius of 1.2 Å. This significant distance variation reflects χ_1 and χ_2 uncertainties of ±20° that still satisfy the measured F−F distance. Varying the backbone tilt angle within the ^{15}N NMR experimental uncertainty does not affect this Trp_{41} constriction. Thus, it is possible that under high pH_{out} and low pH_{in}, the Trp_{41} t90 conformation is such that the pore constriction is at its lower limit of 2.2 Å, which is sufficient to block protons, whereas under low pH_{out}, protonation of the His_{37} imidazole ring may change the Trp_{41} conformation slightly through cation−π interactions[30,31] so that the Trp_{41} constriction opens up to 4−7 Å, allowing protons to pass. The lower-bound constriction may be achieved by Trp_{41} $(\chi_1, \chi_2) \approx (-157°, 110°)$ (Figure 8a), whereas the larger constrictions may be achieved by $(\chi_1, \chi_2) = (163°, 80-90°)$ or $(\chi_1, \chi_2) = (-177°, 70-90°)$ (Figure 8b). Further experiments would be required to ascertain if this conformational change model is correct.

Tetramer Stability and Conformational Heterogeneity in V27F- and L38F-M2TMP. Unlike the Trp_{41} ^{19}F CODEX data, which conclusively show a tetrameric state, the V27F and L38F CODEX intensities both decay to intermediate values of ∼0.4 within the mixing times allowed by the ^{19}F T_1 relaxation time. The L38F data show a clearer decaying trend whereas the V27F intensities appear to have plateaued by 2.0 s. Nevertheless, the V27F data can be fit either to a tetramer−tetramer mixture with different side lengths or to a dimer−tetramer mixture. However, the tetramer−tetramer fit would require Phe_{27} to adopt χ_1 angles differing by 60°. Since residue 27 lies at the *a* position of the heptad repeat and is known to face the pore lumen,[12] we believe this significant side-chain conformation heterogeneity is unlikely. Instead, the V27F mutant may destabilize the helical bundle to partially form dimers or a dimer of dimers that makes up a loose tetramer. In the latter case, the outer dimer may have a $^{19}F-^{19}F$ distance larger than ∼15 Å that cannot be detected in the CODEX experiment. This hypothesis would be consistent with the AUC data[11] showing that the Gibbs free energy of tetramer formation of the V27F mutant is 0.7 kcal/mol higher or less stable than that of the wild-type M2TMP in DPC micelles.[11] The fact that a significant fraction of dimers (50−70%) is observed in lipid bilayers despite the small Gibbs free energy difference may be partly due to intrinsic environmental differences between DPC micelles and lipid bilayers.

In comparison, the CODEX data of the L38F mutant, which is naturally present in the Weybridge virus, is better fit to a tetramer−tetramer mixture. This oligomeric mixture and distance heterogeneity are reasonable because residue 38, unlike residues 27 and 41, faces the lipid molecules,[32] whose thermal disorder can readily affect the side-chain conformation of Phe_{38}. Moreover, residue 38 is close to the center of the helix, thus the phenylene ring lies at a depth near the middle of the bilayer, where the lipid chain disorder is maximal. Thus, a distribution of the Phe χ_1 angle is reasonable. Modeling shows that the F−F distances of 13.1 (58%) and 7.7 Å (42%) are achieved by using χ_1 angles of 180° and −130°, respectively (Supporting Information Figure S6b). The former is the most populated rotamer of Phe in α-helices while the latter is less populated but still found in protein structures at nonnegligible percentages.[26]

Compared to L38F, the Trp_{41} side chain resides largely in the pore lumen except for the end of the six-membered ring (Figure 6c), which points close to the helical interface,[12] thus it is less subject to lipid-induced thermal motion. Trp_{41} is also near the C-terminus of the peptide and thus should be embedded at the membrane−water interface, where the lipid is the most rigid. Thus, conformational heterogeneity should be much reduced at Trp_{41}, as observed by the much lower fraction of a second component (23%) in the best-fit simulation.

To conclusively determine the oligomeric states and fractions of mixtures, additional experiments such as the four-time CODEX experiment are desirable.[5] The main challenge will be to increase the sensitivity of such experiments to make them applicable to membrane-bound peptides and proteins.

The tetramer stability of M2TMP depends not only on the amino acid sequence and site-specific mutations, but also on the membrane environment. DeGrado and co-workers have shown that increasing the lipid chain length and adding cholesterol and amantadine increase the tetramer stability.[16] The presently observed conformational heterogeneity for the V27F and L38F mutants thus may very well change in different membranes. However, this does not change the conclusion that the L38F mutant is relatively stable compared to the V27F mutant in the same membrane.

Conclusion

Interhelical side-chain $^{19}F-^{19}F$ distances have been measured for 5-^{19}F-Trp_{41}, 4-^{19}F-V27F, and 4-^{19}F-L38F positions of M2TMP bound to DMPC bilayers under various conditions. At neutral and acidic pH, the peptide shows the same nearest-neighbor distance of ∼11 Å at Trp_{41}, which is unchanged upon amantadine binding. This distance constrains the Trp_{41} rotamer to t90, and no significant conformational change occurs between the closed and open states. Combined with a previously measured $^{15}N-^{13}C$ distance between His_{37} and Trp_{41}, this suggests that the His_{37} rotamer is t−160 at neutral pH. Gating of the proton channel may be explained either by a cooperative interaction between His_{37} and Trp_{41} that changes the protonation state of the His rings, thus closing or opening the constriction at His_{37}, or by a subtle conformational change of Trp_{41} that changes the pore constriction without affecting the $^{19}F-^{19}F$ distance.

The interhelical $^{19}F-^{19}F$ distances at V27F and L38F are heterogeneous. The V27F mutant data are attributed to a mixture of dimers and tetramers due to the known destabilization of the helical bundle by mutation at this pore-facing site, whereas the data of the naturally occurring L38F mutant are best explained by side-chain conformational heterogeneity of this lipid-facing residue.

Acknowledgment. This work is supported by the National Science Foundation (grant MCB-0543473).

Supporting Information Available: A comparison of the ^{19}F CODEX curves of M2TMP samples prepared with different procedures, model-dependent fitting and rmsd analyses of the Trp_{41} ^{19}F CODEX curves at neutral and low pH, rmsd analyses of the ^{19}F CODEX fitting of V27F and L38F mutants, and the distance−χ_1 angle plot for V27F and L38F mutants. This material is available free of charge via the Internet at http://pubs.acs.org.

References and Notes

(1) Nishimura, K.; Kim, S.; Zhang, L.; Cross, T. A. *Biochemistry* **2002**, *41*, 13170.
(2) Hong, M. *Structure* **2006**, *14*, 1731.
(3) Schmidt-Rohr, K.; deAzevedo, E. R.; Bonagamba, T. J. Centerband-Only Detection of Exchange (CODEX): Efficient NMR Analysis of Slow Motions in Solids. In *Encyclopedia of NMR*; Grant, D. M., Harris, R. K., Eds.; John Wiley & Sons: Chichester, UK, 2002.
(4) deAzevedo, E. R.; Bonagamba, T. J.; Hu, W.; Schmidt-Rohr, K. *J. Am. Chem. Soc.* **1999**, *121*, 8411.
(5) deAzevedo, E. R.; Bonagamba, T. J.; Hu, W.; Schmidt-Rohr, K. *J. Chem. Phys.* **2000**, *112*, 8988.
(6) Luo, W.; Hong, M. *J. Am. Chem. Soc.* **2006**, *128*, 7242.
(7) Buffy, J. J.; Waring, A. J.; Hong, M. *J. Am. Chem. Soc.* **2005**, *127*, 4477.
(8) Lamb, R. A.; Holsinger, K. J.; Pinto, L. H. The Influenza A virus M2 ion channel protein and its role in the influenza virus life cycle. In *Cellular Receptors of Animal Viruses*; Wemmer, E., Ed.; Cold Spring Harbor Lab Press: Plainview, NY, 1994; p 303.
(9) Pinto, L. H.; Lamb, R. A. *J. Biol. Chem.* **2006**, *281*, 8997.
(10) Wang, C.; Lamb, R. A.; Pinto, L. H. *Biophys. J.* **1995**, *69*, 1363.
(11) Howard, K. P.; Lear, J. D.; DeGrado, W. F. *Proc. Natl. Acad. Sci. U.S.A.* **2002**, *99*, 8568.
(12) Pinto, L. H.; Dieckmann, G. R.; Gandhi, C. S.; Papworth, C. G.; Braman, J.; Shaughnessy, M. A.; Lear, J. D.; Lamb, R. A.; DeGrado, W. F. *Proc. Natl. Acad. Sci. U.S.A.* **1997**, *94*, 11301.
(13) Tang, Y.; Zaitseva, F.; Lamb, R. A.; Pinto, L. H. *J. Biol. Chem.* **2002**, *277*, 39880.
(14) Okada, A.; Miura, T.; Takeuchi, H. *Biochemistry* **2001**, *40*, 6053.
(15) Wu, Y.; Voth, G. A. *Biophys. J.* **2005**, *89*, 2402.
(16) Cristian, L.; Lear, J. D.; DeGrado, W. F. *Proc. Natl. Acad. Sci. U.S.A.* **2003**, *100*, 14772.
(17) Pace, C. N.; Vajdos, F.; Fee, L.; Grimsley, G.; Gray, T. *Protein Sci.* **1995**, *4*, 2411.
(18) Liu, W.; Crocker, E.; Siminovitch, D. J.; Smith, S. O. *Biophys. J.* **2003**, *84*, 1263.
(19) Smith, S. O.; Eilers, M.; Song, D.; Crocker, E.; Ying, W.; Groesbeek, M.; Metz, G.; Ziliox, M.; Aimoto, S. *Biophys. J.* **2002**, *82*, 2476.
(20) Lovell, S. C.; Word, J. M.; Richardson, J. S.; Richardson, D. C. *Proteins*: *Struct. Funct. Genet.* **2000**, *40*, 389.
(21) Wang, J.; Kim, S.; Kovacs, F.; Cross, T. A. *Protein Sci.* **2001**, *10*, 2241.
(22) Cady, S. D.; Goodman, C.; Tatko, C. D.; DeGrado, W. F.; Hong, M. *J. Am. Chem. Soc.* **2007**, *129*, 5719.
(23) Harris, N. L.; Presnell, S. R.; Cohen, F. E. *J. Mol. Biol.* **1994**, *236*, 1356.
(24) Sansom, M. S. P.; Kerr, I. D.; Smith, G. R.; Son, H. S. *Virology* **1997**, *233*, 163.
(25) Torres, J.; Kukol, A.; Arkin, I. T. *Biophys. J.* **2001**, *81*, 2681.
(26) Janin, J.; Wodak, S. *J. Mol. Biol.* **1978**, *125*, 375.
(27) Wang, C.; Takeuchi, K.; Pinto, L. H.; Lamb, R. A. *J. Virol.* **1993**, *67*, 5585.
(28) Duff, K. C.; Gilchrist, P. J.; Saxena, A. M.; Bradshaw, J. P. *Virology* **1994**, *202*, 287.
(29) Hu, J.; Fu, R.; Nishimura, K.; Zhang, L.; Zhou, H.-X.; Busath, D. D.; Vijayvergiya, V.; Cross, T. A. *Proc. Natl. Acad. Sci. U.S.A.* **2006**, *103*, 6865.
(30) Gallivan, J. P.; Dougherty, D. A. *Proc. Natl. Acad. Sci. U.S.A.* **1999**, *96*, 9459−9464.
(31) Ma, J. C.; Dougherty, D. A. *Chem. Rev.* **1997**, *97*, 1303.
(32) Stouffer, A. L.; Nanda, V.; Lear, J. D.; DeGrado, W. F. *J. Mol. Biol.* **2005**, *347*, 169.

Supporting Information

Sidechain Conformation of the M2 Transmembrane Peptide Proton Channel of Influenza A Virus from ^{19}F Solid-State NMR

Wenbin Luo, Rajeswari Mani, and Mei Hong*

Department of Chemistry, Iowa State University, Ames, IA 50011

May 17, 2007

Submitted to the *Journal of Physical Chemistry*

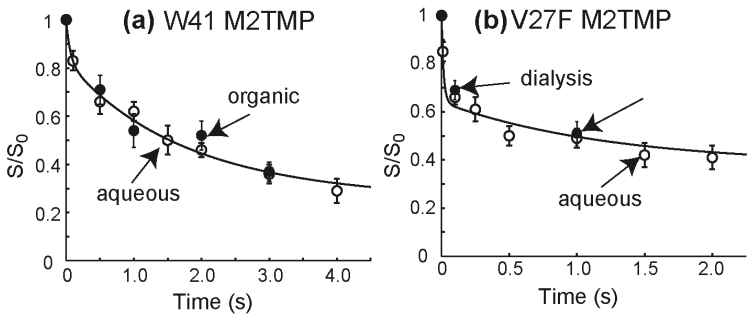

Figure S1. Comparison of ^{19}F CODEX curves for different sample preparation conditions. (a) 5-^{19}F-Trp_{41} labeled M2TMP. The aqueous-phase sample data is shown as open circles and the organic-phase sample data is shown as filled circles. (b) V27F-M2TMP. The aqueous sample data is shown as open circles, while the dialysis sample data is shown as filled circles. No significant differences are observed between the different preparation methods.

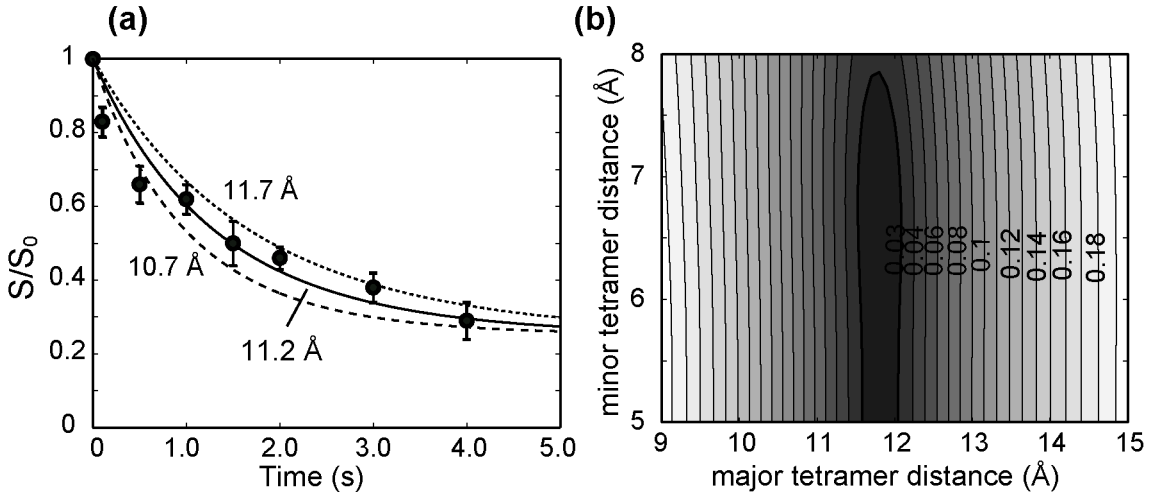

Figure S2. Simulation of the Trp_{41} ^{19}F CODEX data at pH 7.5 using two different models. (a) Simulation using a single-tetramer model. The best-fit interhelical F-F distance is 11.2 ± 0.5 Å. (b) RMSD between the experiment and simulations as a function of the nearest-neighbor distances using a double-tetramer model. The minor and major fractions of the two tetramers are 23% and 77%. The distances giving the minimum RMSD are 11.8 Å for the major component and 6.7 Å for the minor component. Other weight fractions give worse fits.

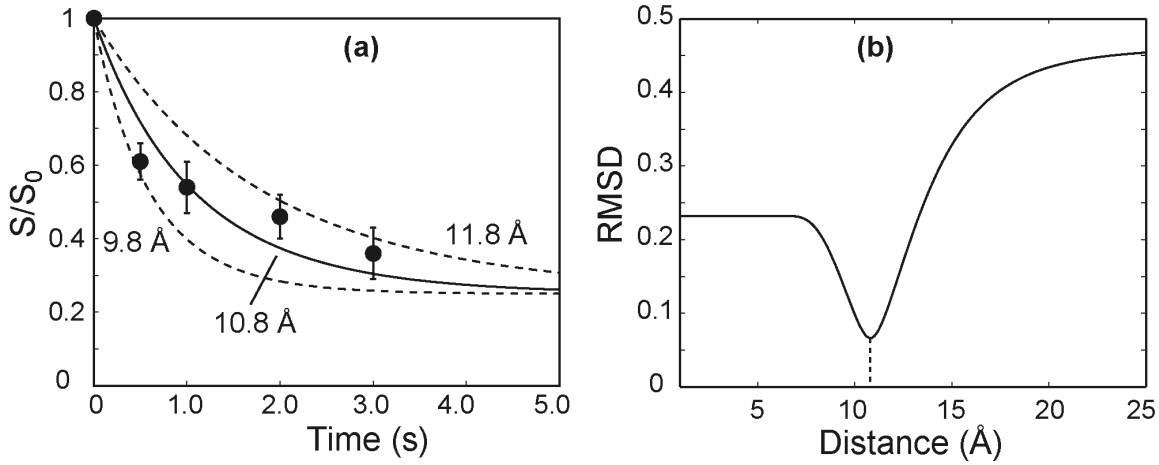

Figure S3. Simulation of the Trp_{41} ^{19}F CODEX data at pH 4.5 using a single tetramer model. (a) The best-fit curve gives a distance of 10.8 Å. Simulated curves for 9.8 Å and 11.8 Å (dashed lines) show the distance uncertainty. (b) RMSD between the simulation and the experiment as a function of the nearest-neighbor F-F distance. The lowest RMSD value is found at 10.8 Å.

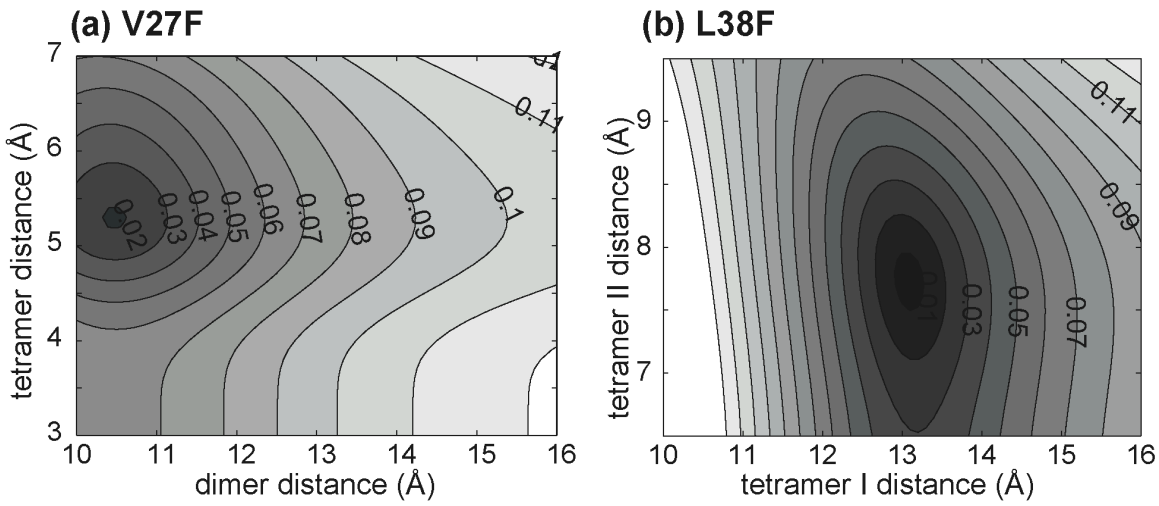

Figure S4. 2D RMSD plots as a function of F-F distances for V27F-M2TMP and L38F-M2TMP. (a) RMSD plot for V27F-M2TMP. A dimer : tetramer mixture with a weight ratio of 52% : 48% is used in the calculation. The lowest RMSD is obtained with a tetramer distance of 5.3 Å and a dimer distance of 10.5 Å. (b) RMSD plot for L38F-M2TMP. A tetramer I : tetramer II mixture at 58% : 42% fractions is used in the calculation. The lowest RMSD value is obtained with a tetramer I distance of 13.1 Å and a tetramer II distance of 7.7 Å.

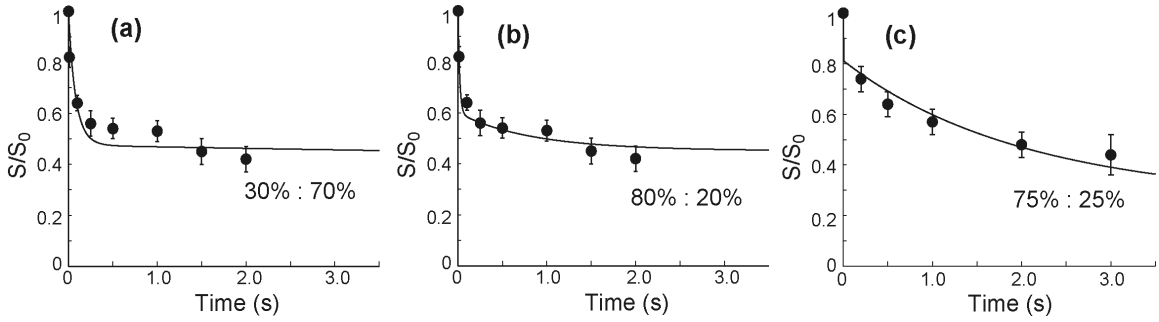

Figure S5. Fitting of the ^{19}F CODEX data of V27F-M2TMP and L38F-M2TMP using different fractions of mixtures. (a) Fitting of the V27F data using a dimer : tetramer model at a ratio of 30:70 gives best-fit distances of 17.1 Å and 7.0 Å. The fit disagrees with the data. (b) Fitting of the V27F data using a dimer : tetramer ratio of 80% : 20% gives best-fit distances of 5.2 Å and 10.4 Å, respectively. The fit deviates from the data at long mixing times. (c) Fitting of the L38F data using a tetramer : tetramer ratio of 75% : 25% gives best-fit distances of 12.1 Å and 1.0 Å. While the fitting is acceptable, the latter distance is unphysical and thus can be ruled out.

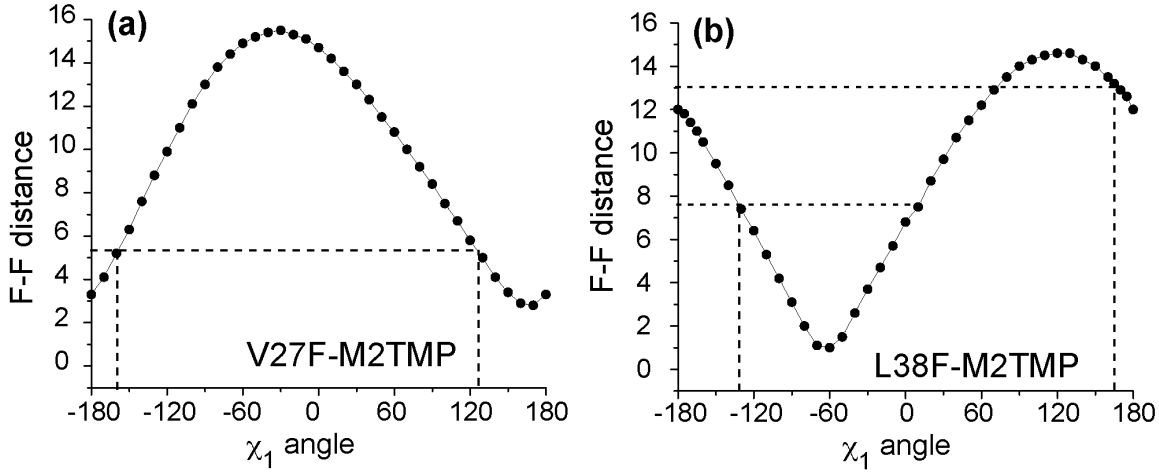

Figure S6. Nearest-neighbor inter-helical F-F distance as a function of Phe χ_1 angle. (a) V27F-M2TMP. The measured F-F distance for the tetramer is 5.3 Å. This is satisfied by a χ_1 angle near the trans conformation. The other solution of ~120° is not a canonical rotamer. (b) L38F-M2TMP. The measured F-F distance in the majority tetramer is 13.1 Å. This corresponds to a χ_1 angle of 180° (the +60° rotamer causes steric conflict with the α-helical backbone). The minor component has a F-F distance of 7.7 Å, which indicates a χ_1 angle of –130°.